Online-Journals.org

iJOE International Journal of Online and Biomedical Engineering

iJOE | eISSN: 2626-8493 | Vol. 21 No. 3 (2025) | OPEN ACCESS

https://doi.org/10.3991/ijoe.v21i03.52305

PAPER

An IoT Monitoring System Based on Artificial Intelligence Image Recognition and EMG Signal Processing for Abdominal Exercise Performance

Marco Jurado, Branco Palma, Andres Figueroa, Guillermo Kemper(✉)

Faculty of Engineering, School of Electronic Engineering, Universidad Peruana de Ciencias Aplicadas, Lima, Perú

guillermo.kemper@upc.pe

ABSTRACT

Correctly executing exercises during training is of vital importance to ensure adequate athletic performance. Sit-ups are among the most frequently performed exercises requiring proper evaluation. This exercise contributes to increasing abdomen strength, having better posture to reduce back problems, and improving overall physical condition and appearance, among other benefits. Existing methods for evaluating the correct execution of sit-ups are manual, subjective, and inefficient in terms of time, cost, and precision. Therefore, there is a need to have technological tools that measure and monitor core abdominal strength while simultaneously verifying, through image processing, the correct execution of the exercise. Since no solutions with these capabilities have been found in the literature, this work proposes a system that performs these functions using electromyographic (EMG) sensors, force signal processing, and biomechanical monitoring based on image processing and the BlazePose algorithm. The results obtained show a very satisfactory performance of the biomechanical monitoring method, where an accuracy of over 95% is obtained in the identification of the correct body posture, while for the estimation of abdominal strength, a sensitivity of over 90% is achieved during the execution of sit-ups.

KEYWORDS

abdominal exercise, electromyographic (EMG) sensors, force measurement, biomechanical monitoring, image processing

1 INTRODUCTION

Scientific and technological studies in the professional field of sports research have continuously evolved, focusing on the development of technological tools that allow obtaining quantitative data. Despite advances in the development of various methods based on wearable inertial sensors to identify simple and repetitive movements,

Jurado, M., Palma, B., Figueroa, A., Kemper, G. (2025). An IoT Monitoring System Based on Artificial Intelligence Image Recognition and EMG Signal Processing for Abdominal Exercise Performance. *International Journal of Online and Biomedical Engineering (iJOE)*, 21(3), pp. 116–141. https://doi.org/10.3991/ijoe.v21i03.52305

Article submitted 2024-09-19. Revision uploaded 2024-12-16. Final acceptance 2025-01-04.

it is still challenging to understand the continuous and complex movements that characterize field sports [1]. For example, accurately determining the resistance and stiffness of a tennis athlete was not possible previously. Currently, efficient and low-cost real-time sports analysis is enabled through the application of motion and vision sensors [2].

On the other hand, the Internet of Things (IoT) is an emerging technology that connects physical devices through the Internet, allowing data to be collected, analyzed, and shared in real time. This network of interconnected devices has applications in diverse areas, including the field of biomechanics and health. IoT plays an essential role in various areas such as healthcare, smart cities, and engineering. Its application allows you to carry out tasks of monitoring, recording, storing, presenting, and communicating information. Using IoT-based monitoring systems, it is possible to track critical health parameters and transmit the data efficiently over the network [3]. Similarly, ecosystems are developed consisting of embedded systems, gateways, smart watches, mobile applications, cloud servers, and control panels. These systems communicate wirelessly, allowing data collected by machines to be transmitted efficiently and comprehensibly to users and sports coaches [4]. The proposed systems employ IoT microcontrollers and devices that significantly improve the accuracy and speed of the entire system. In this way, the IoT has an important impact in the sports field, facilitating the monitoring and preparation of physical performance and well-being. In addition, IoT-enabled devices allow real-time data transmission, allowing athletes and coaches to monitor and evaluate performance indicators, making decisions remotely. Thus, IoT contributes to optimizing training, activities, and performance analysis in sport and health [5].

Consequently, technology has now become a fundamental pillar of the sports industry, particularly in crucial aspects such as improving an athlete's performance, which also implies correctly choosing sensors such as gyroscopes, accelerometers, magnetometers, electrodes, and others [6] so that the information obtained by the sensors can be used to improve the performance statistics of athletes and to optimize the exercises performed to avoid injuries. Then, focusing specifically on the evaluation of the anterior abdominal area of athletes, few existing solutions measure the core abdominal strength using electromyographic (EMG) signals and sensors while simultaneously performing biomechanical monitoring of abdominal exercise through image processing and neural networks, considering that this can give trainers detailed information about the muscles involved and the force applied. This motivated the development of the electronic system proposed in this work, with the aim of generating an important technological contribution to the professional area of sports research.

Furthermore, based on what is indicated in Table 1 and showing relevant information in said table, previous works in the state of the art do not simultaneously measure abdominal muscle strength and monitor biomechanics. Most research focuses on other areas of the body or on prosthesis control via EMG signals. Those works using image processing have a considerable computational load that demands specific hardware capabilities. Also, some investigations require manually storing the sensed information, which creates inefficient and inaccurate records. Moreover, systems do not function in real-time, directly impacting their usefulness since they cannot provide immediate feedback on biomechanics and abdominal strength. Finally, although the works presented had positive results, these were not applied in real scenarios and tested in operation. For this reason, this work seeks to simultaneously use EMG signal monitoring and image processing to adequately determine and evaluate the abdominal exercises performed by athletes.

The most important contributions of this study are listed below:

a) Simultaneity in the estimation of biomechanical movement and the monitoring of EMG signals from the athletes' core muscles, using a camera and precision myoelectric sensors.
b) A system that applies image processing using a pre-trained neural network with a low computational load (BlazePose) for the validation of the biomechanics of abdominal exercise focused on specific points of the region of interest (ROI).
c) High-precision sensing of EMG signals from three muscle groups in the "core" area (upper, lower, and oblique abdominals), which determine the force exerted by the abdomen in the performed exercise.
d) Registration of results in real time on a server and visualization through a mobile application, with the aim that the specialist in the supervision of physical activity can carry out an appropriate and immediate evaluation.

2 MATERIALS AND METHODS

This section describes the design and implementation of the proposed system, in hardware (system components) and software (algorithms for EMG signals, pre-trained neural networks, and image processing).

The chosen materials and methods are the result of a selection process of different experimental tests, environments, levels of operability, computational efficiency, detection of EMG signals, sports, and engineering fundamentals.

Table 1. Research related to muscle strength and biomechanics of the human body

References	Approach	Application	Strengths	Weaknesses
Prakash et al. [7]	Myoelectric prosthesis for detection of EMG signals.	For prosthetic applications.	Compact and affordable.	Oriented only to people with hand amputations.
Romo [8]	Design and development of a system for studying muscles through EMG signals.	Muscular fatigue.	Robust and flexible.	Not field tested, with lack of monitoring of abdominal strength and biomechanics.
Guerrero [9]	Biomechanical monitoring of the human body.	Sensing and measuring through image processing.	Detection of conditions to improve quality of life.	Does not measure abdominal strength simultaneously and works with only one person.
Rui et al. [10]	Comprehensive platform for acquiring biomechanical information of human movement.	Ways to process biomechanical data and ensure synchronization acquisition for different uses.	Innovative biomechanical plate design. Analysis of video capture and EMG technology.	The biomechanical force plate design has a high manufacturing cost.
Bazarevsky et al. [11]	Neural network for human body poses estimation.	Real-time estimation of human pose.	Fitness tracking of human body posture.	It does not store data for analysis and errors occur with two or more users in the neural network.
Zanfir et al. [12]	Neural network that reconstructs the shape and pose of people in 3D.	Reconstruction of the human pose.	Good quality of reconstruction.	High computational load and only valid for one person.
Sarker et al. [13]	Research done for sensing bio signals of the human body.	Acquisition of EMG and ECG signals in 8-channel configuration with 24-bit resolution.	Real-time data transmission. Low consumption.	Only detect signals, without biomechanical monitoring of the human body. Not validated in real applications and with high noise in EMG signals.

(Continued)

Table 1. Research related to muscle strength and biomechanics of the human body *(Continued)*

References	Approach	Application	Strengths	Weaknesses
Kato et al. [14]	Abdominal trunk muscle (ATM) exercise device that measures muscle strength.	Abdominal strength measurement.	Measurement by manual registration. Do not store data in the cloud.	It does not focus on monitoring abdominal strength and exercise biomechanics, and manual work is prone to human errors.
Sharanyanivasini et al. [15]	Integration of biomechanics, cloud computing, and the Internet of Things (IoT).	Analysis of performance and fatigue of athletes in sports training.	Real-time monitoring and access to data in the cloud.	The system uses sensors with low reliability and low sensitivity, in addition to being expensive.
Sangeethalakshmi et al. [16]	Integration of portable sensors and IoT technologies in the field of sport and sports medicine.	Sports performance monitoring.	Collect and analyze real-time data on the athlete's physical condition.	It does not perform validation and evaluation after data collection and has poor readability of the information.
Gehlot et al. [17]	Muscle strength analysis using EMG sensors.	EMG signal reading from the arm of the user or athlete.	Easy implementation and use of a single EMG sensor for monitoring.	Dependence on a desktop computer and not focused on other muscle groups in the body.

2.1 Test environment

For the construction of the test environment, a 1.75 m × 3.00 m gigantography was created and placed on a parallel wall behind the plane where the athlete executed the movements (see Figure 1). The gigantography was designed by drawing reference lines at different angles positioned by a sports specialist. This allowed immediate visual feedback of movements to compare with image processing algorithms. Also, two distances were established to obtain an adequate field of view for image acquisition. The first of them was 3.05 m between the gigantography and the mat (where the athlete is located); the second was 2.00 m between the mat and the tripod, where the image acquisition camera is located, which is at a height of 0.80 m from the floor.

A location for the coach was also established at one end of the mat (see Figure 1), from where he provided instructions, recorded, evaluated, and analyzed the results on the computer and mobile application.

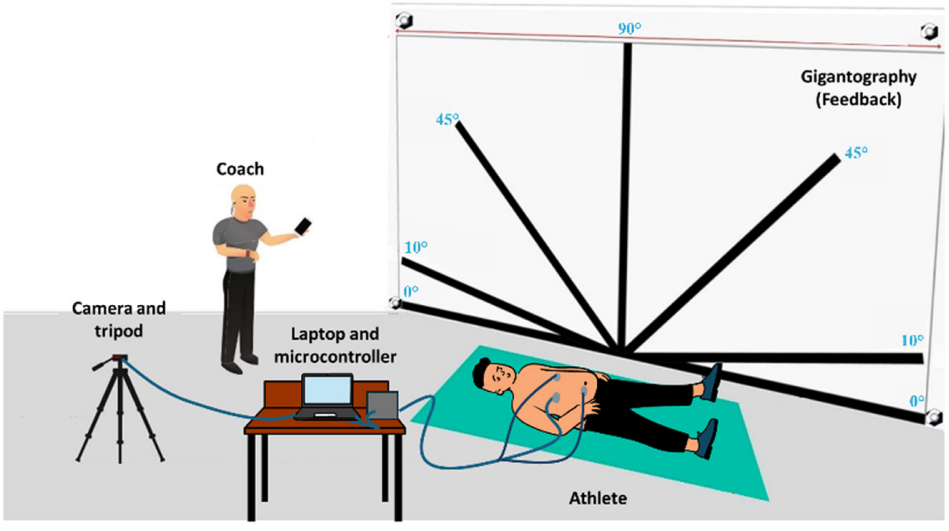

Fig. 1. System test environment distribution

2.2 Athlete preparation

In order to ensure correct data readings, the electrodes required to be adequately adhered to the athlete's abdominal area, which was disinfected prior to executing movements (see Figure 2).

Subsequently, the sensors were located in the three areas of the abdomen: high, low and oblique (see Figure 3), which were linked to a microcontroller connected to a computer for reading data.

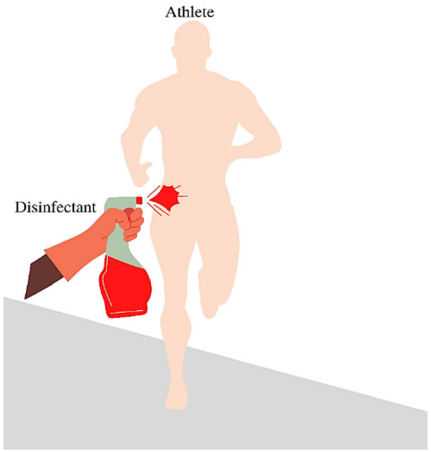

Fig. 2. Abdominal cleaning before placing sensors

2.3 Execution of movements

Two types of abdominal exercise movements were considered: leg lifts (see Figure 4) and trunk lifts (see Figure 5).

For the leg lift to be valid, the athlete must be aligned to the center of the gigantography and lift the legs without taking the buttocks off the ground to reach or exceed 90°. Similarly, to lift the trunk, it must be raised together with the head exceeding the 90° line. If neither case exceeds 90°, the exercise is considered invalid.

When executing the exercise, its intensity grows progressively over a time range. Additionally, the feet, head, and trunk should not completely touch the floor when descending.

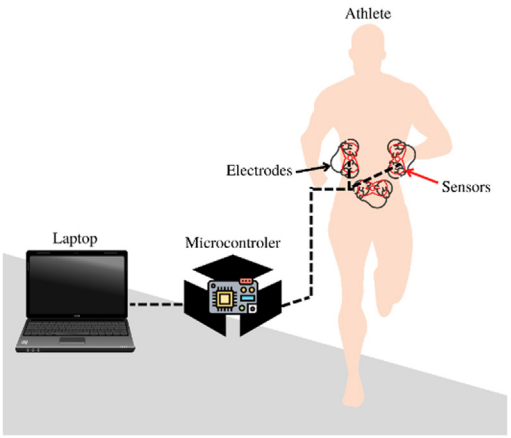

Fig. 3. Sensor location and calibration

2.4 Abdominal force measurement

This section details the implementation process of the electronic device for the acquisition of EMG signals through sensors and surface electrodes. In the sensor circuit, the signal was amplified, filtered, rectified, and then digitized with an A/D converter (analog-to-digital) to obtain the athlete's force data.

Acquisition of EMG signals and obtaining force data. The proposed system used the Myoware sensor with surface electrodes, which acquired and amplified the signals generated by the contraction of the abdominal muscles. This sensor, in addition to amplifying, also filtered and rectified the muscular electrical signal, operating with supply voltages between 2.9 V and 5.7 V. The proposed system used a 5 V supply. In addition, the Myoware incorporates a potentiometer (0.01 Ω to 100 kΩ) to vary the gain depending on the amount of muscle tissue, abdominal fat, and other factors that may alter the signal reading. It has a common mode rejection relationship, or CMRR (common mode rejection ratio), of 110 dB, which guarantees correct amplification, suppressing noise and interference [18].

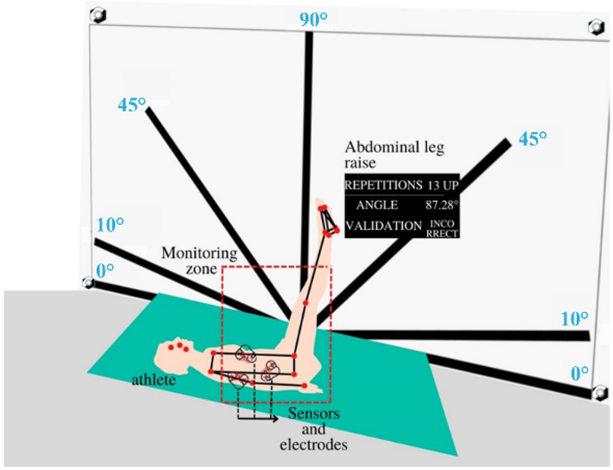

Fig. 4. Abdominal leg lift exercise

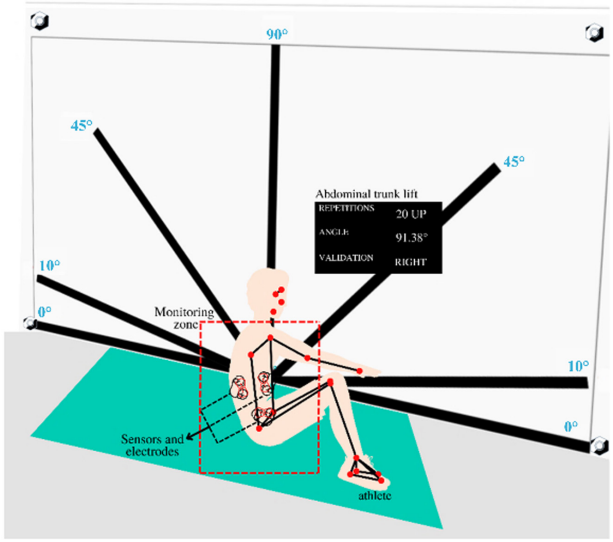

Fig. 5. Abdominal trunk lift exercise

Data was acquired with an ESP32 microcontroller, since it included Wi-Fi connectivity, which permits sending the data wirelessly to a database. Also, it has low-noise A-to-D converters, which allow the reading of the sensor's analog values conversion into numerical data [19]. In addition, it digitizes signals with a resolution of 12 bits per sample, a standard in the measurement of biomedical EMG signals. This resolution results in 4096 quantization levels in a range from 0 V to 5 V, which allows for a minimum quantization error of 0.6 mV [20]. Finally, the ESP32 allows the configuration of the sampling period at T = 250 ms, which implies a sampling frequency value of $f_s = \frac{1}{T} = 4\,\text{Hz}$ (samples per second).

Figure 6 shows the electronic diagram of the signal sensing (EMG signal acquisition, A/D conversion, battery charging system, and data display on an OLED screen).

Figure 7 shows the block diagram of the signal processing executed by the Myoware sensor. First, it performs a preamplification in order to increase the input signal voltage level, including noise and frequency components from adjacent muscles [21]. Second, the sensor performs filtering that eliminates the greatest amount of noise because the frequencies of the EMG signals are usually below 100 Hz [22], so the sensor is configured with low-pass and high-pass first-order filters with frequencies between 20 Hz and 500 Hz and a filter that eliminates line frequency noise. Although filters eliminate noise, they may also distort the waveform of EMG signals. Thus, the sensor has a full-wave rectifier that converts the output wave with a constant polarity [23].

The final stage has an inverter amplifier where a clean EMG signal without noise is obtained, whose amplification is adjustable through a potentiometer as shown in the following expression:

$$G = 201 \times \frac{R_{gain}}{1\text{k}\Omega} \tag{1}$$

Where:

- G: Adjustable gain
- R_{gain}: Variable resistance (Ω)

Finally, the obtained signal is digitized by and stored in the ESP32 microcontroller.

Equation 2 [24] shows the A/D conversion equation resulting from the digitization in the microcontroller, considering a 12 bits resolution and a 5 V supply voltage.

$$L_{AD}(nT) = \text{round}\left(\frac{V_{AM}(nT) \times R_{AD}}{V_{AS}}\right) \tag{2}$$

Where:

- n: Integer index that identifies the time position of a sample (n = 0, 1, ….).
- T: Sampling period.
- R_{AD}: A/D converter resolution.
- $L_{AD}(nT)$: Digital readout of A/D converter at time t = nT.
- V_{AS}: System supply voltage.
- $V_{AM}(nT)$: Measured analog value at time t = nT.

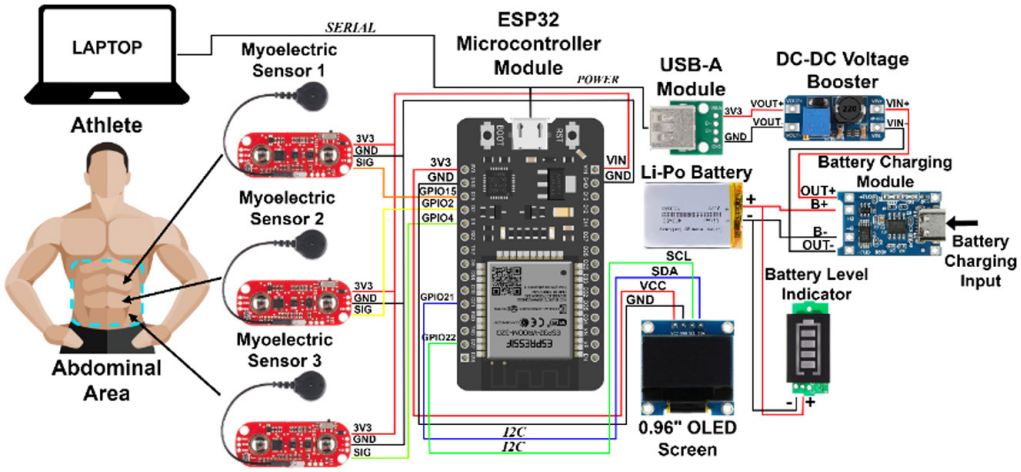

Fig. 6. Electronic diagram of the acquisition stage of the EMG signal

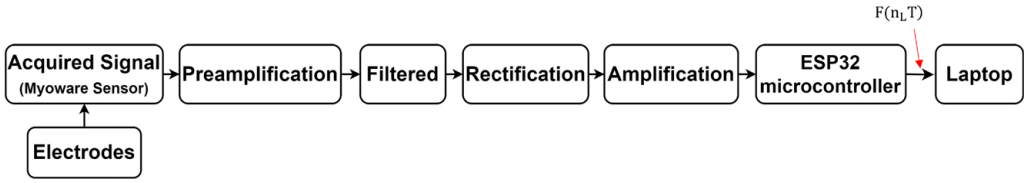

Fig. 7. Block diagram of the signal acquisition stage

Data are then obtained from 3 muscle zones, where a simple arithmetic averaging is executed, which does not involve a high computational load and provides good stability in data sampling [25]; also, this provides us a measure of central tendency (see equation 3) of the data obtained by the three Myoware sensors.

$$L_{A_{PF}}(nT) = \frac{L_{AD_{S1}}(nT) + L_{AD_{S2}}(nT) + L_{AD_{S3}}(nT)}{3} \quad (3)$$

Where (see Figure 6):

- $L_{AD_{S1}}(nT)$: Digital reading of sensor 1 at time, t = nT
- $L_{AD_{S2}}(nT)$: Digital reading of sensor 2 at time, t = nT
- $L_{AD_{S3}}(nT)$: Digital reading of sensor 3 at time, t = nT
- $L_{A_{PF}}(nT)$: Final averaged digital reading at time, t = nT

With equation 4, a single final voltage of the three Myoware sensors are obtained after performing the abdominal exercise.

$$V_{PF}(nT) = \frac{L_{A_{PF}}(nT) \times V_{AS}}{R_{AD}} \quad (4)$$

Where:

- $V_{PF}(nT)$: Final average voltage at time, t = nT

The voltage-force relation was estimated from graphs and tables [7] relating muscle contraction, strength, and voltage. Figure 8 shows this relationship.

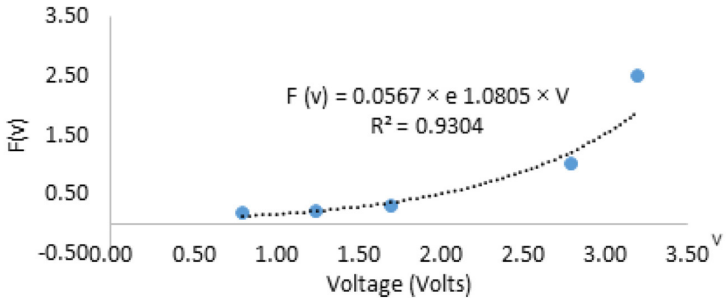

Fig. 8. Voltage vs. force model graph

From the curve shown in Figure 8, we obtain finally the force value $F(n_{L_0}T)$ in newtons based on the average voltage obtained at measurement time $t = n_L T$ from the EMG sensors:

$$F(n_L T) = 0.0567 \times e^{1.0805(V_{PF}(n_L T))} \quad (5)$$

The described procedure can be applied for both types of sit-ups: abdominal legs and abdominal trunk.

It is also important to indicate that the process from A/D conversion to obtaining the force value is executed in the ESP32 microcontroller.

Analysis for abdominal series with different difficulty levels. In some cases, for evaluation purposes, it is necessary to know the average force exerted by the athlete's abdomen when performing a certain number of consecutive sit-ups (series) with an assigned level of difficulty. This difficulty consists of adding weights (from 0 to 5 kg) on the legs (leg abdominals) or held with the hands on the trunk (trunk abdominals) in order to generate greater effort when executing the exercise and evaluate the athlete's performance.

For a series of NA abdominals, we obtain the average effective voltage $V_{ef}(n_L T)$ obtained at measurement time $t = n_L T$

$$V_{ef}(n_L T) = \sqrt{\frac{1}{NA} \times \sum_{i=1}^{NA} V_{PF}^2(n_i T)} \quad (6)$$

Where:

- $n_i T$: Measurement time in which the $V_{PF}(n_i T)$ voltage samples are obtained and recorded (this is given when the biomechanical monitoring detects a certain value or angular condition in the abdominal executed)
- $V_{ef}(n_L T)$: Average effective voltage of an abdominal series obtained at measurement time, $t = n_L T$
- NA: Number of sit-ups performed in a series

Tables 2 and 3 show the values obtained in a series for the abdominal leg lifting exercise, and for the trunk lifting exercise respectively (for different difficulty levels with extra weights applied). With this data and applying the multiple linear regression method, equations 7 and 8 were obtained to relate the average effective voltage $V_{ef}(n_L T)$ emitted by the sensors and the average force $F_{ef}(n_L T)$ exerted by the athlete at measurement time, $t = n_L T$.

Table 2. Effective tabbing abdominal legs

W_1	NA	$V_{ef}(n_LT)$	$F_{ef}(n_LT)$
0	27	4.213	5.374
1	21	4.316	6.011
2	19	4.325	6.070
3	17	4.466	7.065
4	10	4.468	7.087
5	8	4.473	7.122

$$F_{ef}(n_LT) = -22.830 + 0.039 \times W_1 + 0.008 \times NA + 6.639 \times V_{ef}(n_LT) \quad (7)$$

Table 3. Effective tabbing abdominal trunk

W_1	NA	$V_{ef}(n_LT)$	$F_{ef}(n_LT)$
0	22	4.526	7.537
1	19	4.524	7.523
2	17	4.464	7.050
3	16	4.605	8.214
4	12	4.637	8.503
5	9	4.630	8.435

$$F_{ef}(n_LT) = -29.733 + 0.013 \times W_1 + 0.001 \times NA + 8.229 \times V_{ef}(n_LT) \quad (8)$$

Where:

- W_1: Extra weights from 0 to 5 kg

It is important to indicate that the values obtained and shown in Tables 2 and 3 were generated by an outstanding athlete in optimal physical conditions, so they may be considered as reference points for future evaluations and validations.

2.5 Biomechanical monitoring

Biomechanical monitoring was carried out through a pre-trained real-time image recognition algorithm based on artificial intelligence to detect the different postures and angles (BlazePose) that were generated during the execution of abdominal exercises. The algorithm has three stages (see Figure 9): image acquisition and cropping (stage 1), image processing (stage 2), and rendering and determination of angles (stage 3).

It is important to point out that all the stages of the biomechanical monitoring algorithm are executed on the laptop that is part of the system, which will read from the microcontroller the value of the force detected at the moment of obtaining the angles of the executed exercise (simultaneous measurement).

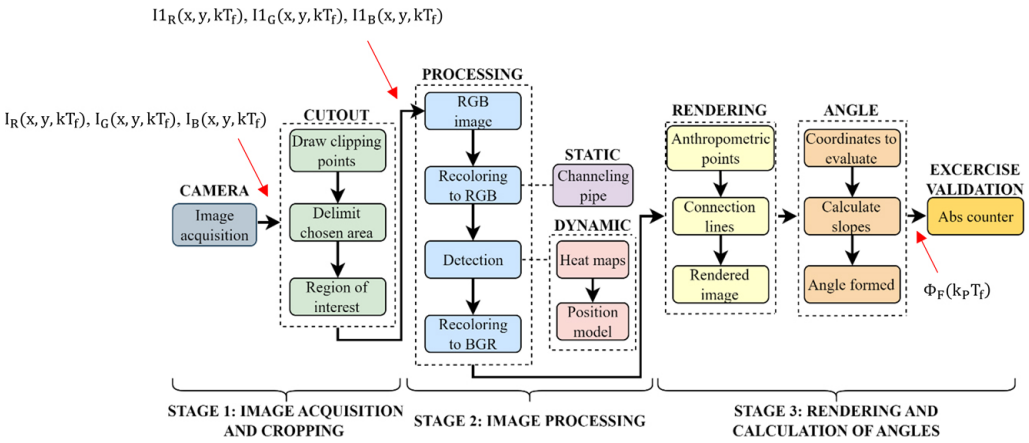

Fig. 9. Biomechanical monitoring block diagram

Stage 1: Image acquisition and cropping. Image acquisition is performed by configuring video capture in 720p format, frame rate f_r = 30 frames per second and resolution of N = 1280 (columns) and M = 720 (rows). Each acquired frame can be expressed through its primary RGB components; $I_R(x, y, kT_f)$, $I_G(x, y, kT_f)$, and $I_B(x, y, kT_f)$, where (x, y) are the spatial coordinates, "k" the integer index (k = 0, 1, ….) that identifies the temporal position of a frame at time $t = kT_f$ and T_f the frame time with value $T_f = \frac{1}{f_r} = \frac{1}{30} = 33.33\,\text{ms}$.

For the indicated resolution we also have that x = 0, 1, …, M–1, and, y = 0, 1, …, N–1.

The acquisition area of the image encompasses the athlete and the person providing support during the execution of the abdominal exercise (see Figure 10). A ROI is obtained in the previously described image, which contained only the athlete executing the exercise. Cropping reduced computational load and reduced errors by ensuring the presence of only one person in the scene for the calculation of the angles with the pose estimation algorithm.

The cropped image can be expressed as, $I1_R(x, y, kT_f)$, $I1_G(x, y, kT_f)$, and $I1_B(x, y, kT_f)$ with a resolution of M1 rows and N1 columns (in this case we have that M1 ≤ M and N1 ≤ N). The ROI was configurable by the user through a visual interface.

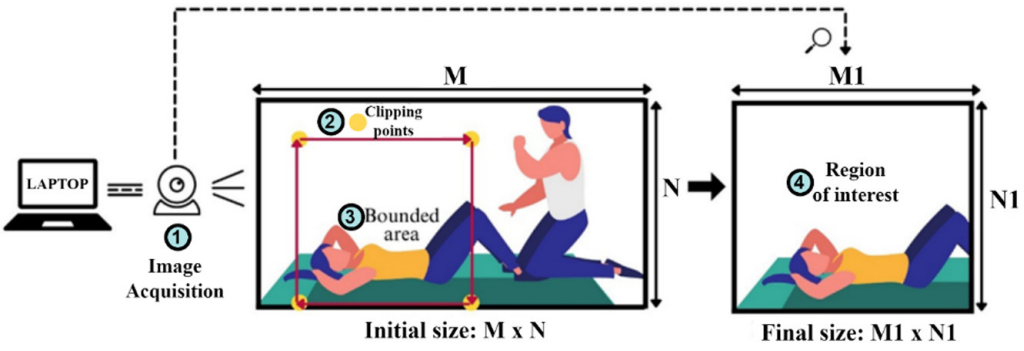

Fig. 10. Pictorial diagram of stage 1 of the biomechanical monitoring algorithm

Stage 2: Image processing. Initially, at this stage, each frame expressed as $I1_R(x, y, kT_f)$, $I1_G(x, y, kT_f)$, and $I1_B(x, y, kT_f)$ is recolored for subsequent analysis with OpenCV (see Figure 9).

Then, for detection during static and dynamic moments (execution of exercises), a channeling tube was used, applying machine learning as a detector-tracker tool [11, 26].

Using the detector, the channeling first locates the ROI containing the position of the person within the frame. Subsequently, the tracker predicts the positional landmarks within the ROI using the cropped frame as input. The channeling is implemented as a MediaPipe graph using a 3-dimensional module pose landmark subgraph (see Figure 11) and is represented using a dedicated pose-rendered subgraph [26].

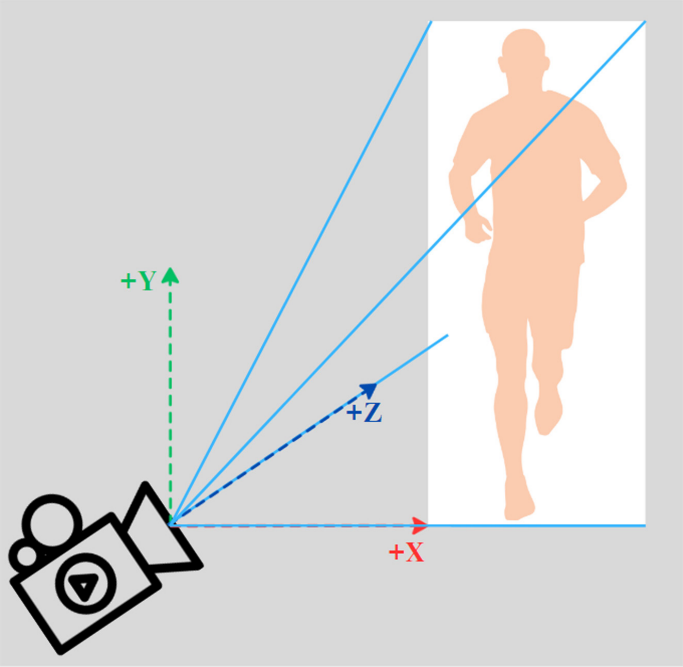

Fig. 11. Position reference point subgraph [26]

Next, image detection and processing were carried out using the pre-trained neural network BlazePose, in which a re-colorized image was obtained as output to perform pixel ordering. The person's face and body were segmented in a lower and upper region, respectively. Thus, the encoder-decoder network model was trained to predict the heat maps for all joints. Then, by combining the position model with the skeleton joint center prediction function, the total shape of the body was obtained by joining the previously separated body and face and showing them as a skeleton. The previously obtained heat maps are traversed using the ReLU activation function. If the ReLU output is greater than zero, this is interpreted as the person moving in a particular region (seen as a stain in Figure 12). The region's position is later updated with the next positions in the executed movement, in order to take the referential anthropometric points [27].

Stage 3: Rendering and determining the angles. The Euclidean distances were used to update skeletal joint centers, joining the anthropometric points (see Figure 12) together with the predictor (see Figure 13), where the line colors indicate a certain area of the body. The heat maps and the model skeleton of the anthropometric points were fused, thus estimating the three-dimensional coordinates (X, Y, Z) from the movement and the heat map values in each position [28].

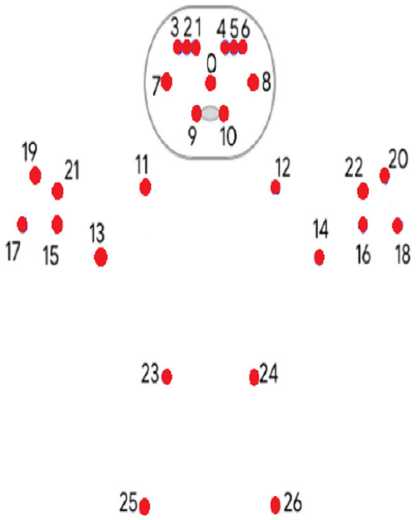

Fig. 12. Anthropometric points of the body

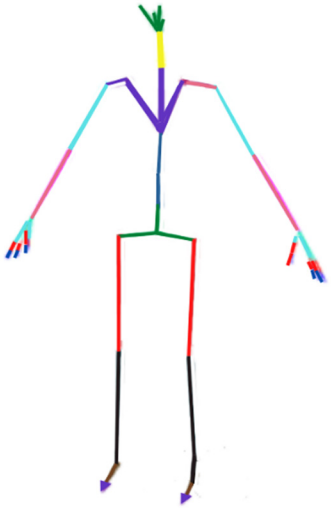

Fig. 13. Joint model of the body

The rendered image with 33 anthropometric points (see Figure 14) was obtained, but only three of them were taken to determine the angles in the abdominal exercise. A BGR image was re-colorized to reduce the computational load [11].

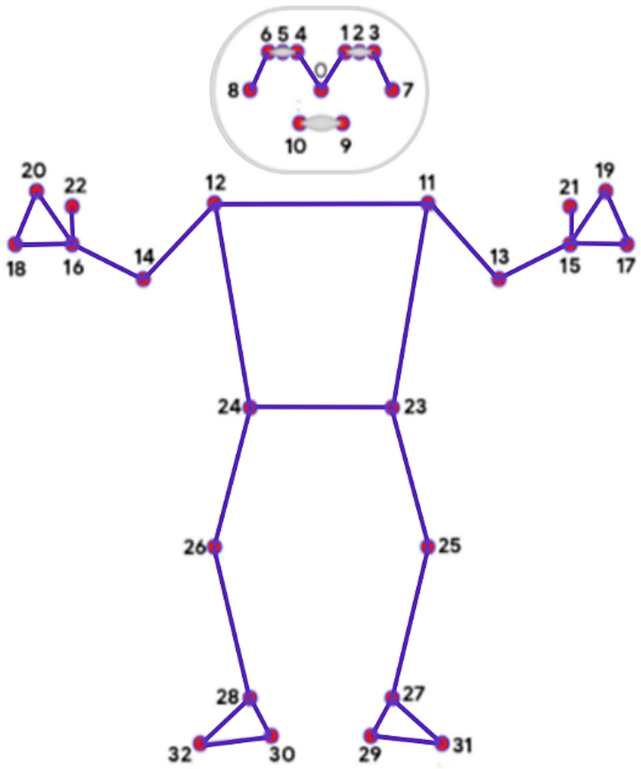

Fig. 14. Rendered image of the body

The angle formed by the three aforementioned points were used to calculate the angle (see Figure 15).

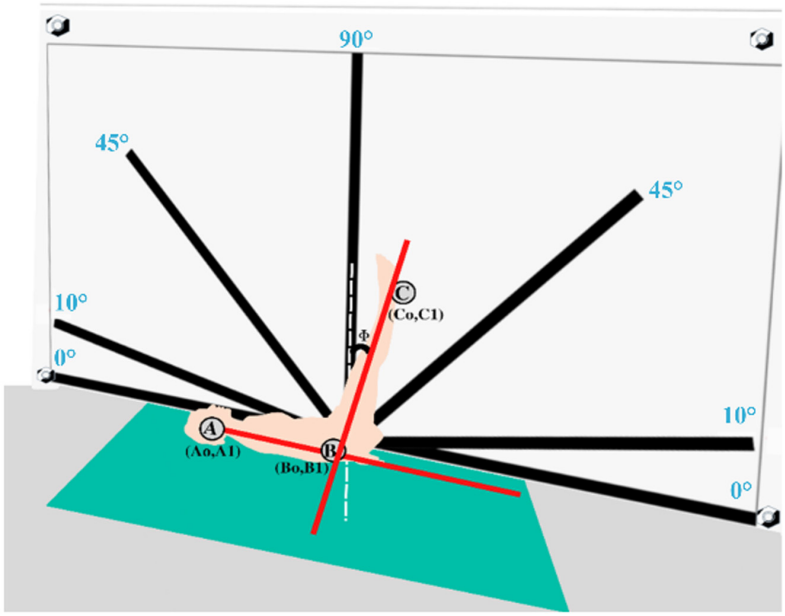

Fig. 15. Calculated angle points

Equation 10 was used to compute the angle (in radians) between points C and B forming the line with slope $m\overline{CB}(k_pT_f)$ at frame time $t = k_pT_f$:

$$m\overline{CB}(k_pT_f) = \left(\frac{C_1(k_pT_f) - B_1(k_pT_f)}{C_0(k_pT_f) - B_0(k_pT_f)}\right) \tag{9}$$

$$\Phi_1(k_pT_f) = \tan^{-1}(m\overline{CB}(k_pT_f)) \tag{10}$$

Equation 12 was used to perform a similar computation but using point A and B forming the line with slope $m\overline{AB}(k_pT_f)$ at frame time $t = k_pT_f$:

$$m\overline{AB}(k_pT_f) = \left(\frac{A_1(k_pT_f) - B_1(k_pT_f)}{A_0(k_pT_f) - B_0(k_pT_f)}\right) \tag{11}$$

$$\Phi_2(k_pT_f) = \tan^{-1}(m\overline{AB}(k_pT_f)) \tag{12}$$

Equation 13 shows the calculation of the final angle $\Phi_S(k_pT_f)$ in sexagesimal degrees. The absolute value ensures that the angle is always positive:

$$\Phi_S(k_pT_f) = \text{round}\left(\left|\left(\frac{180}{\pi} \times (\Phi_1(k_pT_f) - \Phi_2(k_pT_f))\right|\right)\right) \tag{13}$$

$$\Phi_F(k_pT_f) = \begin{cases} \Phi_S(k_pT_f) & , \ \Phi_S(k_pT_f) \le 180° \\ 60° - \Phi_S(k_pT_f) & , \ \Phi_S(k_pT_f) > 180° \end{cases} \tag{14}$$

The angle $\Phi_S(k_pT_f)$ is converted to the range 0° to 180° through equation 14, resulting in angle $\Phi_F(k_pT_f)$.

2.6 Simultaneous measurement of force and angles

Figure 16 shows the operation of the proposed system, visualizing the stages and processes of image and EMG signal acquisition.

Simultaneity is achieved when biomechanical monitoring and abdominal muscle force detection are carried out together. This implies that the force exerted by the abdomen should be measured and recorded at the same instant when angular values or conditions are detected through biomechanical monitoring. Therefore, the simultaneous measurement time t_{SM} must satisfy the following condition:

$$t_{SM} = k_p T_f = n_L T \tag{15}$$

This will allow evaluating the correspondence between exerted force and generated angle in the same time instant, which will give more elements of judgment to the coach or supervisor of the athlete.

The following list details the steps required to take a set of samples during an exercise:

- Step 1: Preparation of the stage and athlete.
- Step 2: The athlete's data (ID, name, age, weight, and height) is recorded on the mobile device and sent to the database server.
- Step 3: Data verification is performed on the mobile device and the database.
- Step 4: The athlete is located and positioned correctly in the defined areas. Simultaneously, the abdominal area is cleaned to place the Myoware with the electrodes.
- Step 5: The webcam is connected to a laptop that executed the computer vision algorithm. At the same time, the EMG sensors are placed to proceed to connect them with the microcontroller ESP32 and then with a laptop to receive the abdominal force data.
- Step 6: The stopwatch is set to 1 minute (execution time for each abdominal series), and biomechanics are monitored through image processing, and simultaneously, abdominal force signal processing is performed.
- Step 7: Once the exercises have finished, all the running applications are manually paused. Next, the results of monitoring biomechanics and abdominal force are obtained.
- Step 8: The lists of values are obtained (athlete data, number of total sit-ups, number of correct and incorrect sit-ups, and abdominal strength value), whose data are stored in real time on the implemented server.
- Step 9: Finally, data is stored in the mobile device to validate and verify the results obtained from biomechanical and abdominal force monitoring.

2.7 Data logging and results display

Figure 17 presents a diagram showing the data transmission and reception route of the proposed system. First, the athlete's data is recorded in the mobile application, performing a validation that ensures the storage of values. Second, the biomechanical monitoring data is stored since it is captured and processed by a laptop.

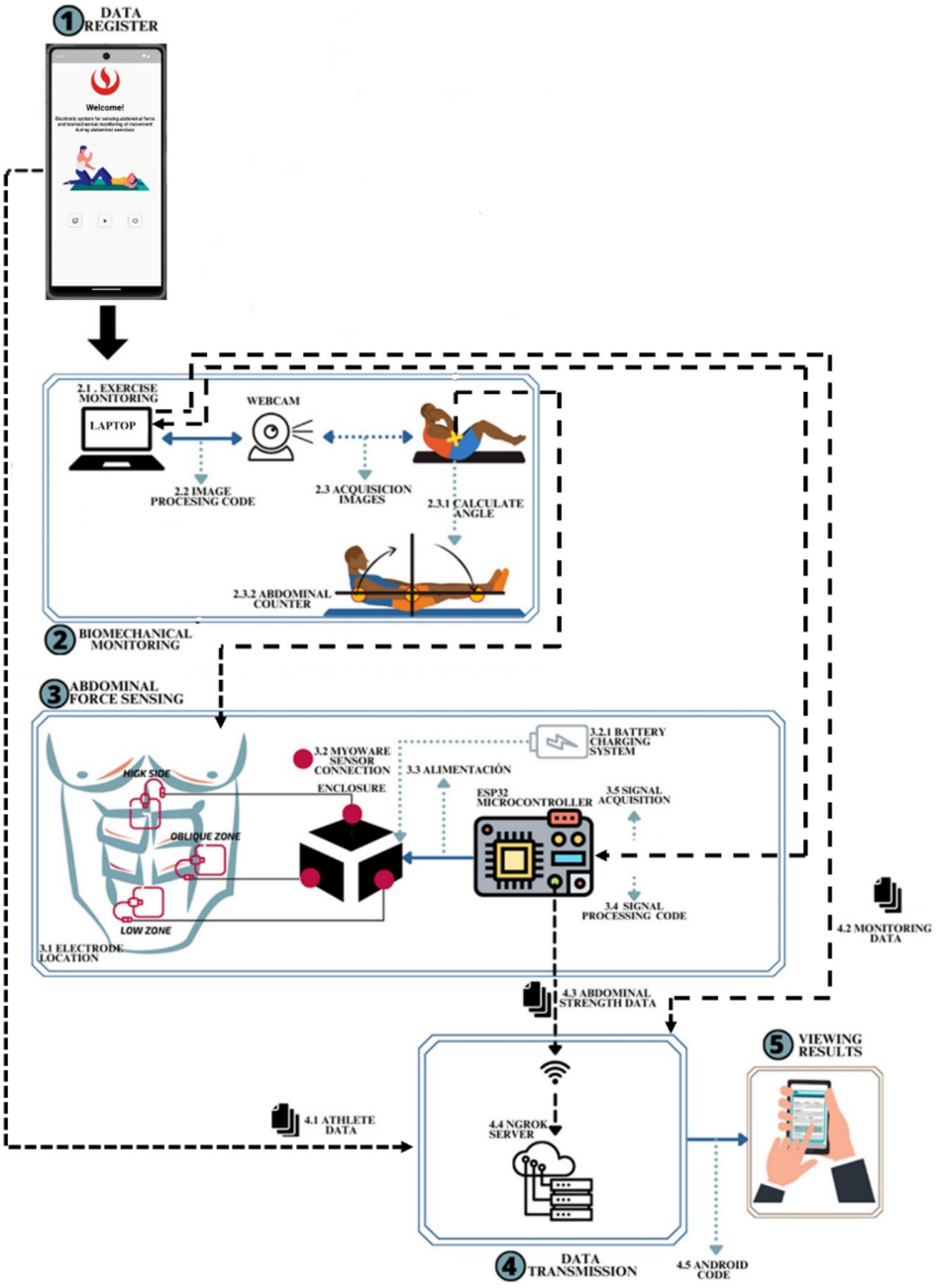

Fig. 16. Pictorial representation of the proposed system

Next, the abdominal muscle force data stored in the ESP32 microcontroller is sent to the server, connected wirelessly with the phpMyAdmin data manager and managed from a laptop with the implemented web server. Finally, laptop connects to an Azure [28] service and sends data to the cloud.

Figure 18 presents the route for displaying results in the interface on an Android mobile device. A "Welcome" screen is followed by a "Menu" screen, where users may choose between registering a new athlete and viewing an existing one's history. Once the athlete has completed their evaluation, they have the option to choose the movement that will be recorded in their history. Finally, the user may choose which athlete has been evaluated from a list, as well as view the total number of exercises in order to evaluate the efficiency and average strength of the three evaluated areas.

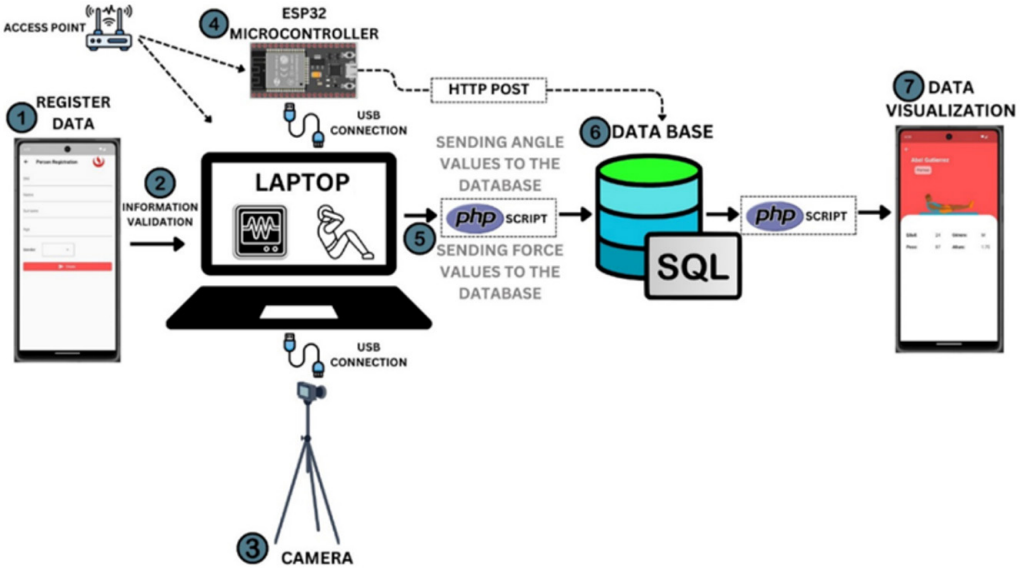

Fig. 17. Pictorial data transmission diagram

Fig. 18. Mobile application interface and results

3 RESULTS AND DISCUSSION

This section describes the validation procedure and the obtained results in the performance tests of the proposed system. Two performance variables have been validated: correct detection of the formed angles and correct validation of the performed exercise.

3.1 Detection of formed angles

To validate the system's angle detection, the obtained ones were compared with those obtained through visual measurement using a reference gigantography with angles for visualization (see Figure 19).

The angles were obtained as the athlete raised and lowered their trunk and legs since the neural network measures the different angles that are formed at all times.

Table 4 shows the validation criteria, where correct/incorrect criteria were defined by a specialized sports coach.

The error expressed in equation 16 was the validation metric. The 90° determined by the coach in all repetitions are considered the correct angle, and they are compared with the angle obtained by the processing system to obtain an angle error value (A_e) expressed as:

$$A_e = A_{ref} - A_{obt} \tag{16}$$

Where:

- A_{ref}: Reference angle (≥ 90° is the angle of an exercise performed correctly)
- A_{obt}: Angle obtained through the proposed system

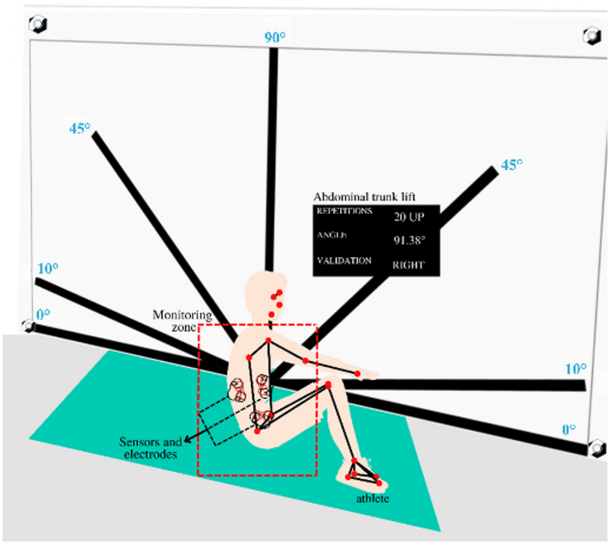

Fig. 19. Comparison of proposed algorithm and gigantography

Table 4. Angle validation table [29]

Angle Formed	Abdominal Exercise		A_e
	Leg Lift	Trunk Lift	
≥90°	Correct	Correct	Negative value
<90°	Incorrect	Incorrect	Positive value

Data on the formed angles for trunk and leg abdominals were recorded for 10 athletes (three athletic and seven common people) for a period of 1 minute. The results of the three most outstanding athletes are shown in Figures 20, 21, and 22 for the leg lift exercise. Likewise, the results of the abdominal trunk lift exercise are shown in Figures 23, 24, and 25.

In the 3 cases (Figures 20, 21, and 22), the repetitions are valid, since the performed leg lift exceeds the 90° angle mark. Consequently, it can be determined that for this exercise the 3 athletes have optimal abdominal strength.

Figures 23, 24, and 25 show variations in the detected angle value, which is expected due to physical fatigue. All repetitions with angles less than 90° are considered incorrect.

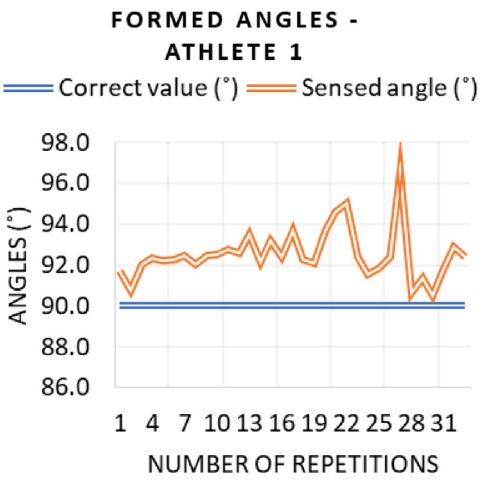

Fig. 20. Graph of formed angles – Athlete legs 1

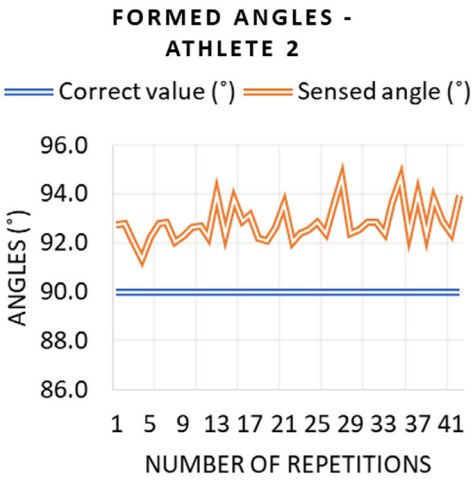

Fig. 21. Graph of formed angles – Athlete legs 2

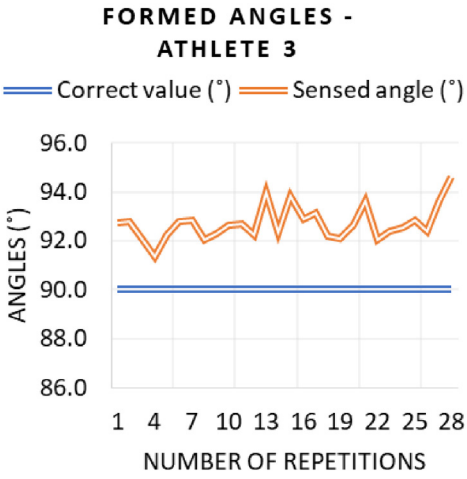

Fig. 22. Graph of formed angles – Athlete legs 3

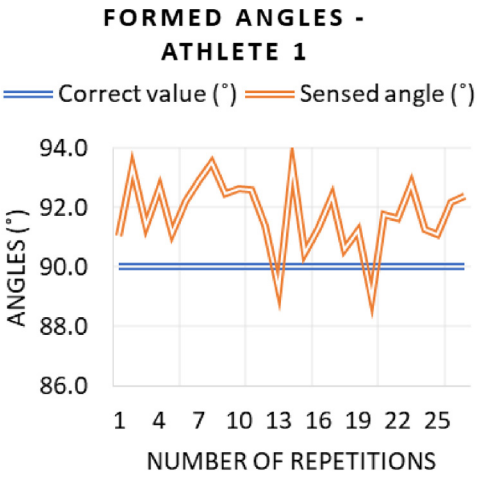

Fig. 23. Graph of formed angles – Athlete trunk 1

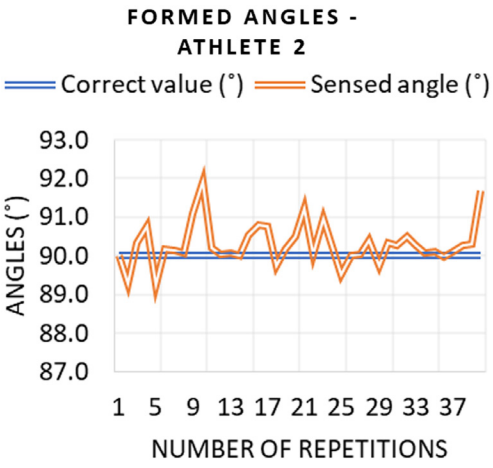

Fig. 24. Graph of formed angles – Athlete trunk 2

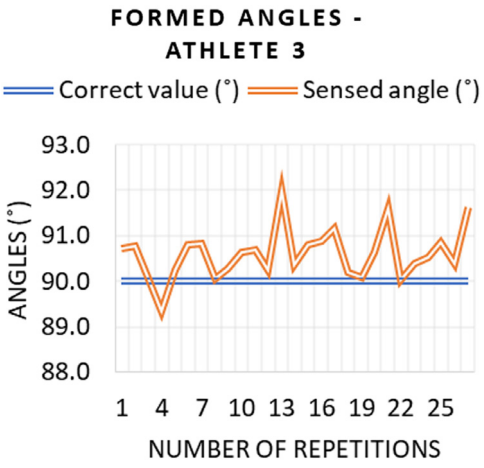

Fig. 25. Graph of formed angles – Athlete trunk 3

Therefore, it is determined that due to the complexity in the estimation of the anthropometric points necessary to validate the angle formed in the abdominal trunk lift, the reliability of the pre-trained neural network model turns out to be a valuable tool. This algorithm and neural network are able to estimate the angle, which is traditionally measured through visual perception supported by gigantography.

3.2 Validation of correctly executed exercises

To validate the correct execution of exercises, each athlete participating in the test performed trunk and leg abdominal exercises for one minute. The proposed system measured the voltage and thus the applied force during the ascending and descending phases of the exercise.

Simultaneously with the force measurement, the image processing and angle detection algorithm was executed. The voltage and force values where the athlete formed an angle greater than 90° were selected. Table 5 shows the ranges established to define the athlete's condition [29] (also taking as reference the values obtained in Tables 2 and 3 with some tolerance).

Table 5. Results validation table for abdominal strength [29]

Condition	V_{ef}	F_{ef}
very developed	≥ 4.50	≥ 7.33
developed	4.10–4.49	4.76–7.32
underdeveloped	≤ 4.09	≤ 4.75

The results obtained for the three most outstanding athletes in the abdominal exercise of trunk lifting and leg lifting are shown in Tables 6 and 7, respectively. The procedure applied to obtain the force values is similar to that described in section 2.4.2.

Table 6. Abdominal force results – Legs

Athlete	Extra Weight (kg)	n° Repetitions	V_{ef}	F_{ef}
1	0	33	4,015	2,770
2	0	42	4,365	5,997
3	0	28	3,890	1,620

Table 7. Abdominal force results – Trunk

Athlete	Extra Weight (kg)	n° Repetitions	V_{ef}	F_{ef}
1	0	27	4,050	4,553
2	0	40	4,565	7,448
3	0	27	3,990	4,209

Figures 26, 27, and 28 (validation of correctly executed exercises – leg raises) show three cases where the angles exceeded 90°. In this case, a negative error was obtained, meaning that the repetitions were correctly executed.

Figures 29, 30, and 31 (validation of correctly executed angles – trunk lift) show angle values smaller than 90°, which means that certain repetitions are incorrect.

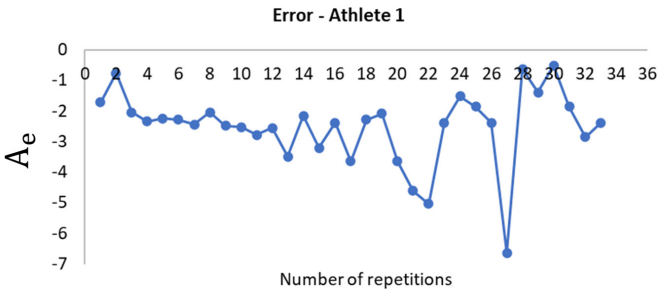

Fig. 26. Leg repetition error graph – Athlete 1

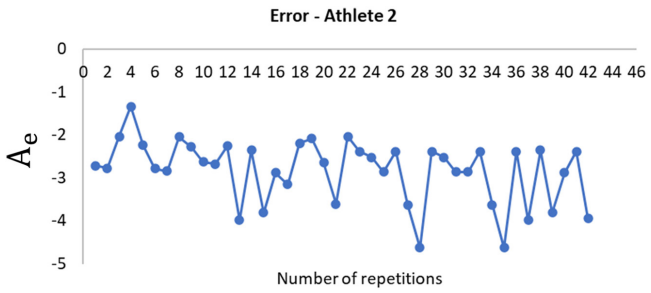

Fig. 27. Leg repetition error graph – Athlete 2

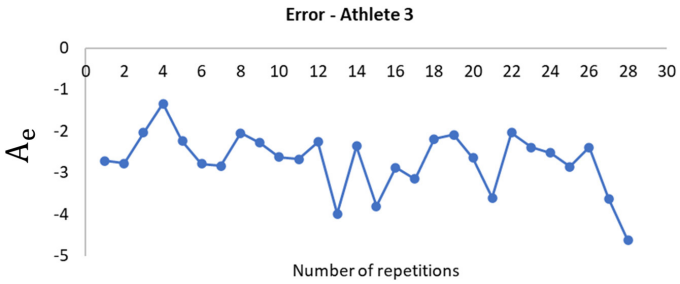

Fig. 28. Leg repetition error graph – Athlete 3

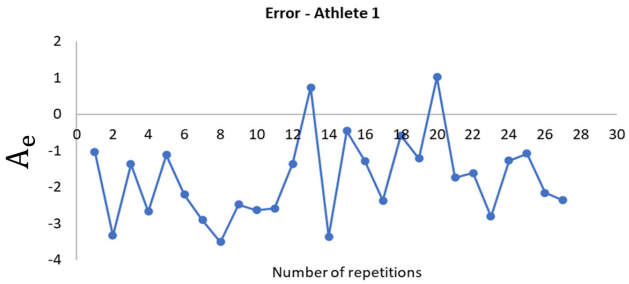

Fig. 29. Trunk repetition error graph – Athlete 1

Fig. 30. Trunk repetition error graph – Athlete 2

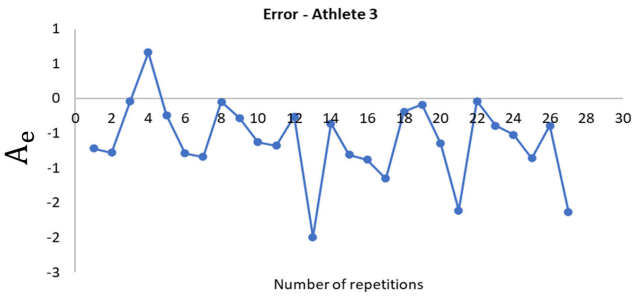

Fig. 31. Trunk repetition error graph – Athlete 3

Testing verifies that the number of performed sit-ups influences the abdominal force results, since with more repetitions it is expected that abdominal strength will increase.

Additionally, the correct measurement of abdominal force is highly sensitive to the correct placement of sensors and electrodes on the athlete's abdomen. To achieve this, the abdominal area must be properly cleaned and disinfected before placing electrodes and EMG sensors. This reduces the probability of obtaining erroneous data, minimizes interference from adjacent muscles, and prevents electrode disconnection.

Correct posture and proper execution of exercises are critical factors that contribute to obtaining accurate values in measuring abdominal force. Proper posture ensures that the abdominal muscles are activated optimally, avoiding muscular compensations that could alter the results. Additionally, proper exercise execution ensures that movements are performed in the proper range and sequence, which is essential for reliable measurement of muscle activity.

In the three analyzed cases, certain repetitions did not exceed 90°, most likely due to the difficulty level of the exercise and the athlete's abdominal strength capacity. Likewise, according to Figures 27 and 30, athlete 2 achieved greater average abdominal strength in both exercises. This information is corroborated with the numerical value of force in Newtons presented in Tables 6 and 7. Also, Figures 27 and 30 confirm that the effective voltage obtained by the sensors has a directly proportional relationship to the abdominal force exerted by the abdomen.

Unlike previous works, this solution does not require a computer with expensive software licenses such as Matlab and Toolbox for the processing of the signals obtained by the EMG sensors. A clean signal can be obtained with the Myoware sensor without requiring further pre-processing, in contrast to the solution proposed in Romo [8]. Furthermore, although in Guerrero [9] a correct measurement of angles was achieved using OpenCV as a library, the validation scenario only took into account the angles formed by the knees, hip, and ankle without considering electromyographic measurements.

On the other hand, the research carried out by Hu [10] obtained good results for estimating people's posture, but it required using a steel plate with 6 axes to measure the applied force, which makes the solution not applicable to all scenarios and with serious difficulties for transportation.

Moreover, the results from using the BlazePose Lite model achieved higher FPS (frame per seconds) compared to algorithms such as OpenPose, despite the fact that according to Table 8 the algorithm has lower precision in the detection of anthropometric points (PCK) with an error of less than 20% for the test datasets such as people in nature (AR Data) and people performing yoga (Yoga Data).

Table 8. Comparison of detection algorithms [11]

Model	FPS	AR Data PCK@0.2	Yoga Facts PCK@0.2
OpenPose (Body Only)	0.4	87.8	83.4
BlazePose Full	10	84.1	84.5
BlazePose Lite	31	79.6	77.6

4 CONCLUSIONS AND FUTURE WORK

The proposed system achieved an efficiency greater than 95% in computing angles and validating exercises through image processing, while its sensitivity was greater than 90% when sensing abdominal muscle force.

In general, it was possible to implement an electronic system that provides a simultaneous evaluation method with greater precision and speed for biomechanical monitoring and abdominal force measurement during the execution of two types of abdominal exercises. In this way, quantifiable, precise data and an economical option are provided compared to similar products.

The 95% efficiency resulted from comparing the model running on a computer with a visual inspection technique, obtaining a maximum of two counting errors in each performed repetition.

Using the metrics in Tables 4 and 5, the exercise angle, correct/incorrect execution of the exercises, and abdominal muscle strength were validated. The abdominal strength measurement during trunk lifting showed a force close to 8 N (effective voltage greater than 4.5 V), and during leg lifting resulted in a force

of approximately 5 N. The validation of correctly executed exercises with angles greater than 90° corresponded to force values close to the aforementioned ones.

Future work includes automatically determining the region of interest before applying the detection models. Additionally, more robust algorithms may be developed, being less susceptible to the athlete's environments and enabling them to locate them in places with random backgrounds and at variable distances from the camera.

Other limitations of the system include the need for a controlled light environment and that the distance between the athlete and the camera must be fixed to work. Additionally, this system can only be used on one athlete at a time, and if more people appear in the shot, false detections could occur.

The electronic system is designed to obtain a precise muscle signal, optimizing the performance and physical resistance of athletes, which will contribute to strengthening the core in athletes and prevent future injuries in the abdominal area. Additionally, by targeting the core muscles of the body, it improves stability and balance, reducing the likelihood of injuries during sports practice.

The proposed system may be used by physical therapy and rehabilitation professionals. Moreover, it may be calibrated to different sports, therapeutic or rehabilitation procedures, which makes it a valuable tool, contributing to the recovery of muscle injuries, improvement of muscle function, and aiding in the rehabilitation process related to the core muscles.

5 ACKNOWLEDGMENT

The authors would like to thank the Dirección de Investigación of Universidad Peruana de Ciencias Aplicadas, Lima, Peru, for funding and logistical support.

6 REFERENCES

[1] L. Huang, H. Ma, W. Yan, W. Liu, H. Liu, and Z. Yang, "Sports motion recognition based on foot trajectory state sequence mapping," in *International Joint Conference on Neural Networks (IJCNN)*, Budapest, Hungary, 2019, pp. 1–8. https://doi.org/10.1109/IJCNN.2019.8851921

[2] C. Zhang, F. Yang, G. Li, Q. Zhai, Y. Jiang, and D. Xuan, "MV-Sports: A motion and vision sensor integration-based sports analysis system," in *IEEE Conference on Computer Communications*, Honolulu, HI, USA, 2018, pp. 1070–1078. https://doi.org/10.1109/INFOCOM.2018.8485910

[3] B. G. Mohammed and D. S. Hasan, "Smart healthcare monitoring system using IoT," *International Journal of Interactive Mobile Technologies*, vol. 17, no. 1, pp. 141–152, 2023. https://doi.org/10.3991/ijim.v17i01.34675

[4] S. Bian, A. Rupp, and M. Magno, "Fully automatic gym exercises recording: An IoT solution," in *2023 IEEE International Workshop on Metrology for Industry 4.0 & IoT (MetroInd4.0 & IoT 2023)*, Brescia, Italy, 2023, pp. 310–314. https://doi.org/10.1109/MetroInd4.0IoT57462.2023.10180177

[5] R. Raman, M. Kaul, R. Meenakshi, S. Jayaprakash, D. Rukmani Devi, and S. Murugan, "IoT applications in sports and fitness: Enhancing performance monitoring and training," in *2023 2nd International Conference on Smart Technologies for Smart Nation (SmartTechCon)*, Singapore, 2023, pp. 137–141. https://doi.org/10.1109/SmartTechCon57526.2023.10391301

[6] A. Kos, A. Umek, S. Tomazic, and Y. Zhang, "Identification and selection of sensors suitable for integration into sport equipment: Smart golf club," in *Proceedings – 2016 International Conference on Identification, Information and Knowledge in the Internet of Things (IIKI),* Beijing, China, 2016, pp. 128–133. https://doi.org/10.1109/IIKI.2016.71

[7] A. Prakash, S. Sharma, and N. Sharma, "A compact-sized surface EMG sensor for myoelectric hand prosthesis," *Biomedical Engineering Letters*, vol. 9, no. 4, pp. 467–479, 2019. https://doi.org/10.1007/s13534-019-00130-y

[8] A. Romo, "Diseño De Un Sistema Para El Análisis De Señales Dinámicas Electromiográficas En Estudios De Ergonomía Basado En Técnicas Temporales Y Frecuenciales," Tesis De Master, Universitad Politécnica de Valencia, 2021. [Online]. Available: http://hdl.handle.net/10251/159590

[9] P. N. Guerrero, "Análisis Biomecánico Del Cuerpo Humano Mediante El Procesamiento Digital De Imágenes," Tesis De Grado, Universidad Tecnológica Nacional, 2018. [Online]. Available: https://ria.utn.edu.ar/items/ed1e31f1-61e4-4a66-aadc-bb8603b29695

[10] R. Hu, R. Dong, and Y. Tang, "A comprehensive biomechanical information acquisition platform for human motion," in *2018 IEEE 4th Information Technology and Mechatronics Engineering Conference (ITOEC)*, Chongqing, China, 2018, pp. 726–730. https://doi.org/10.1109/ITOEC.2018.8740403

[11] V. Bazarevsky, I. Grishchenko, K. Raveendran, T. Zhu, F. Zhang, and M. Grundmann, "BlazePose: On-device real-time body pose tracking," *arXiv preprint arXiv:arxiv.2006.10204*, 2020. https://doi.org/10.48550/arxiv.2006.10204

[12] A. Zanfir, E. G. Bazavan, M. Zanfir, W. T. Freeman, R. Sukthankar, and C. Sminchisescu, "Neural descent for visual 3D human pose and shape," in *IEEE Computer Society Conference on Computer Vision and Pattern Recognition (CVPR),* Nashville, TN, USA, 2021, pp. 14479–14488. https://doi.org/10.1109/CVPR46437.2021.01425

[13] V. K. Sarker, M. Jiang, T. N. Gia, A. Anzanpour, A. M. Rahmani, and P. Liljeberg, "Portable multipurpose bio-signal acquisition and wireless streaming device for wearables," in *2017 IEEE Sensors Applications Symposium (SAS)*, Glassboro, NJ, USA, 2017, pp. 1–6. https://doi.org/10.1109/SAS.2017.7894053

[14] S. Kato *et al.*, "Reliability of the muscle strength measurement and effects of the strengthening by an innovative exercise device for the Abdominal trunk muscles," *Journal of Back and Musculoskeletal Rehabilitation*, vol. 33, no. 4, pp. 677–684, 2020. https://doi.org/10.3233/BMR-181419

[15] J. S. Sharanyanivasini, M. Nirmalprithivraj, S. Tharanipriya, G. Pradeepkumar, M. M. Arun Prasath, and R. Saravanakumar, "Sports applications of biomechanics wearable sensors using IoT," in *Proceedings of the 2023 2nd International Conference on Electronics and Renewable Systems (ICEARS),* Tuticorin, India, 2023, pp. 613–618. https://doi.org/10.1109/ICEARS56392.2023.10085068

[16] K. Sangeethalakshmi, C. Sasi Kumar, V. V. Lakshmi, S. Giriprasad, N. Malathi, and S. Velmurugan, "Smart biomechanics system with IoT and Cloud computing for injury prevention and muscle fatigue analysis," in *2023 3rd International Conference on Smart Generation Computing, Communication and Networking (SMART GENCON),* Bangalore, India, 2023, pp. 1–5. https://doi.org/10.1109/SMARTGENCON60755.2023.10442220

[17] A. Gehlot *et al.*, "Real time monitoring of muscle fatigue with IoT and wearable devices," *Computers, Materials and Continua*, vol. 72, no. 1, pp. 999–1015, 2022. https://doi.org/10.32604/cmc.2022.023861

[18] Sparkfun, "3-lead Muscle / Electromyography sensor for microcontroller applications," *Advancer Technologies*, 2015. [Online]. Available: https://cdn.sparkfun.com/datasheets/Sensors/Biometric/MyowareUserManualAT-04-001.pdf

[19] Espressif, "ESP32-DevKitC," docs.espressif.com, 2024. [Online]. Available: https://docs.espressif.com/projects/esp-idf/en/latest/esp32/hw-reference/esp32/get-started-devkitc.html

[20] J. A. Alarcón, L. E. Ruiz, and J. L. Tello, "Diseño e Implementación De Un Sistema De Adquisición Y Procesamiento De Señales Mioeléctricas Para El Reconocimiento En Tiempo Real De La Contracción De Los Bíceps Y Tríceps Braquiales Orientado a La Manipulación De Un Brazo Robótico De Tres Grados De Libertad," Tesis De Grado, Universidad Peruana de Ciencias Aplicadas (UPC), 2014. [Online]. Available: http://hdl.handle.net/10757/322724

[21] R. Farfan, "Implementación De Un Dispositivo De Detección De Señales Electromiográficas Para El Monitoreo De La Actividad Muscular," Tesis De Grado, Universidad Tecnológica del Perú, 2021. [Online]. Available: https://hdl.handle.net/20.500.12867/4869

[22] M. Renuka, B. Divya, and B. Preethi, "Active low pass filter for biomedical applications," *International Journal of Engineering Sciences & Research Technology*, pp. 214–223, 2017. https://doi.org/10.5281/zenodo.1116616

[23] P. López, "Diseño E Implementación De Un Sistema EMG De Captación De Señales Musculares Y Su Aplicación a Un Sistema Robótico," Tesis De Grado, Universitat Politècnica de València, 2021. [Online]. Available: https://proxy.europeana.eu/media/355/https___hispana_mcu_es_lod_oai_riunet_upv_es_10251____173632_ent0/48886f13edb-70c862ff3afa1de92a4b8?disposition=inline&recordApiUrl=https%3A%2F%2Fapi.europeana.eu%2Frecord

[24] Freescale Semiconductor, Inc., "How to increase the analog-to-digital converter accuracy in an application," nxp.com, 2016. [Online]. Available: https://www.nxp.com/docs/en/application-note/AN5250.pdf

[25] J. Rodríquez, "Significado De La Media Aritmética Y El Uso De La Palabra Promedio Para Los Estudiantes De Grado Undécimo De Una Institución Educativa De Ibagué," Tesis De Grado, Universidad del Tolima, 2018. [Online]. Available: https://repository.ut.edu.co/server/api/core/bitstreams/9ef1da41-ffff-4ab9-b0b1-4dccc184aafe/content

[26] MediaPipe and Google, "Pose landmark detection guide," Google Developers, 2019. [Online]. Available: https://developers.google.com/mediapipe/solutions/vision/pose_landmarker

[27] H. Xu, E. G. Bazavan, A. Zanfir, W. R. Freeman, R. Sukthankar, and C. Sminchisescu, "GHUM & GHUML: Generative 3D human shape and articulated pose models," in *IEEE Computer Society Conference on Computer Vision and Pattern Recognition (CVPR),* Seattle, WA, USA, 2020, pp. 6183–6192. https://doi.org/10.1109/CVPR42600.2020.00622

[28] Microsoft, "Qué Es Azure: Servicios En La Nube De Microsoft," Microsoft.com, 2022. [Online]. Available: https://azure.microsoft.com/es-es/resources/cloud-computing-dictionary/what-is-azure/

[29] G. Moscoso Otoya, "Tables validation communication," *Emotional experiences,* vol. 24, no. 2, pp. 136–141, 2021. https://doi.org/10.1037/hop0000182

7 AUTHORS

Marco Jurado received a B.S. degree in Electronic Engineering with mention in Telecommunications and Management and Leadership in 2021 from the Peruvian University of Applied Sciences (UPC), Lima, Peru. He has worked at the National Institute for Research and Training in Telecommunications (INICTEL-UNI) in projects of environmental monitoring, water quality and greenhouse gas monitoring,

related to IoT and embedded systems. Currently, he is working on projects related to signal processing and data transmission with GPRS technology and SIGFOX technology. His research interests include signal processing, embedded systems, IoT, hardware design, and artificial intelligence.

Branco Palma received his B.S. degree in Electronic Engineering from the Peruvian University of Applied Sciences (UPC). His main interests are based on network and telecommunications engineering, monitoring and control of networks and telecommunications and technical support of networks. Currently, he is working in technical support and monitoring of FTTH Internet networks and telecommunications.

Andres Figueroa earned his B.S degree in Electronic Engineering from the Peruvian University of Applied Sciences (UPC), Lima, Peru, in 2021. Early in his career, he was part of a telecommunications support operation team, where he gained valuable experience in maintaining and optimizing communication systems. Currently, he is dedicated to developing new telecommunication services for the Business-to-Business (B2B) segment and researching emerging technology trends in the industry. His research interests include image processing, embedded systems, and telecommunications.

Guillermo Kemper received his BS degree in electronic engineering from Universidad Privada Antenor Orrego de Trujillo, Peru, in 1994 and his MS and PhD degrees in electronic engineering in the areas of telecommunications and telematics from the State University of Campinas, São Paulo, Brazil, in 1996 and 2001, respectively. He is currently a full-time research professor at the School of Electronic Engineering, Universidad Peruana de Ciencias Aplicadas, Lima, Peru, and an IEEE senior member. His line of research focuses on digital signal and image processing with emphasis on digital television, biomedical engineering, remote sensing and precision agriculture among others (E-mail: guillermo.kemper@upc.pe).